

# METHOD OF ESTIMATION FOR FLOOD DISCHARGES CAUSED BY OVERFLOW EROSION OF LANDSLIDE DAMS AND ITS APPLICATION IN AS A COUNTERMEASURE

Toshio MORI<sup>1</sup>, Tetsuo SAKAGUCHI<sup>1</sup>, Youji SAWA<sup>1</sup>  
Takahisa MIZUYAMA<sup>2</sup>, Yoshifumi SATOFUKA<sup>3</sup>  
Kiichiro OGAWA<sup>4</sup>, Nobuhiro USUKI<sup>4</sup>, Kousuke YOSHINO<sup>4</sup>

## ABSTRACT

When a landslide dam forms, it is essential at an early stage to estimate the flood discharge generated by overflow erosion, which is known to be the most common pattern for a dam to burst, as well as to promptly discuss emergency measures for reducing the flood discharge and to put a warning and evacuation system in place for residents in the downstream areas. This report describes the result of the application of the “two-layer model” suggested by Takahama et al. (Takahama et al., 2000) to the overflow and burst phenomena of the Tangjiashan landslide dams formed due to the Wenchuan Earthquake in May 2008. Moreover, it describes model sensitivity analysis of the flood discharge volume reducing effect of excavating landslide dams crown and makes model study on effective means of reducing the value of flood discharges caused by overflow erosion of landslide dams.

**Key Words:** landslide dam, outburst, flood discharge, two-layer model, risk-analysis

## INTRODUCTION

The impact of the bursting of landslide dams on flood discharge is a very important factor from the standpoint of preventing secondary disasters. However, not many studies or reports have been made on specific flood data, although a large number of cases of such bursts have been reported. For this reason, only modest progress has been made in research in this field up to now. The authors examined in detail the literature on a study of a flood caused by landslide dams that formed and burst on the Naka River in Tokushima Prefecture Japan in 1892, confirmed that this study had a certain level of reliability and attempted a simulation with the “two-layer model.” As a result of these efforts, the flood level was successfully approximated to some extent (Mizuyama et al., 2006; Satofuka et al., 2007a).

Next, a flood caused by landslide dams that formed and burst on the Mimi River in Miyazaki Prefecture Japan in 2005 was simulated using the records of outflow and inflow data of the

---

1 Director General, Sabo Frontier Foundation, Sabo-kaikan, Hirakawa-cho 2-7-4, Chiyoda-ku, Tokyo 102-0093 (Corresponding Author; Tel.: +81-3-5216-5871; Fax: +81-3-3262-2201; [rijicyou@sff.or.jp](mailto:rijicyou@sff.or.jp))

2 Professor, Graduate School of Agriculture, Kyoto University, Oiwake-cho, Kitashirakawa, Sakyo-ku, Kyoto 606-8502 ([mizuyama@kais.kyoto-u.ac.jp](mailto:mizuyama@kais.kyoto-u.ac.jp))

3 Professor, College of Science and Engineering Department of Civil Engineering, Ritsumeikan University, Noji-higashi 1-1-1, Kusatsu-city, Shiga 525-8577 ([satofuka@se.ritsumei.ac.jp](mailto:satofuka@se.ritsumei.ac.jp))

4 Asia Air Survey C.,Ltd. Shinyuri 21 Bldg., 1-2-2 Manpukuji, Asao-ku, Kawasaki-city, Kanagawa 215-0004 ([ki.ogawa@ajiko.co.jp](mailto:ki.ogawa@ajiko.co.jp), [usu.usuki@ajiko.co.jp](mailto:usu.usuki@ajiko.co.jp))

power company dams in the upstream and downstream areas and so on, which succeeded in producing an approximate match (Chiba et al., 2007; Satofuka et al., 2007b). Consequently, the authors have decided that the “two-layer model” is an adequate model for analyzing overflow burst phenomena associated with landslide dams.

In the Wenchuan Earthquake that occurred in May 2008, 35 landslide dams were formed counting the major ones alone. Based on information obtained via the Internet on one of those dams, called the Tangjiashan landslide dam, in the upper reaches of the Jianjiang River in Sichuan Province, the authors attempted a simulation, the successful result of which was to produce a general match with the actual phenomenon.

In addition, in the case of the Tangjiashan landslide dam, it proved possible to reduce flood level by excavating the crown of the dam. As a result of a model study in which varying depths and widths of excavation were applied, we confirmed that deep excavation was an effective means of reducing the flood level resulting from an overflow burst.

### The “two-layer model” used in the calculation

For analysis of the transition process from a debris flow to a bed load transport-like collective flow, Takahama et al. (Takahama et al., 2000) focused on the essential difference in the constitutive law between the water flow layer and the gravel moving layer and suggested the “two-layer model” with an analysis based on a governing equation for each layer. The two-layer model analyzes the governing equation for each layer based on the conservation law resulting from the introduction of the water flow flux through the interface between the water flow and the gravel moving layers and the momentum flux according to the velocity vector of the interface, which is described in Figure 1. This model is applicable continuously to every phenomenon from debris flow to bed road transport. Volumetric values of the water layer per units of time and area through the interface are defined as  $s_I$ . And Satofuka et al. (Satofuka et al., 2007b, 2007c) adopted governing equations for  $ss_T$  defined as erosion velocity of torrent side bank.

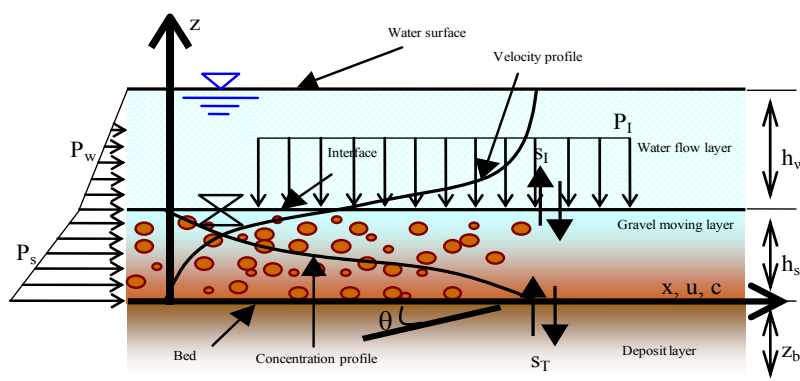


Fig. 1 The two-layer model (Takahama et al., 2000, partially revised)

### Continuous equations

(1) Water flow layer

$$\frac{1}{B_I} \frac{\partial B h_w}{\partial t} + \frac{1}{B_I} \frac{\partial B v_w h_w}{\partial x} = s_I + 2s s_T \frac{h_{w1}}{B_I} \quad (1)$$

(2) Gravel moving layer

$$\frac{1}{B_1} \frac{\partial B h_s}{\partial t} + \frac{1}{B_1} \frac{\partial B v_s h_s}{\partial x} = s_T - s_I + 2ss_T \frac{h_{s1}}{B_1} \quad (2)$$

(3) Sediment continuous equations in gravel moving layer

$$\frac{1}{B_1} \frac{\partial c_s B h_s}{\partial t} + \frac{1}{B_1} \frac{\partial \gamma c_s B v_s h_s}{\partial x} = c_* \left( s_T + 2ss_T \frac{h_{s1}}{B_1} \right) \quad (3)$$

(4) Temporal change of torrent bed elevation

$$\frac{\partial z_b}{\partial t} = -s_T \frac{B_1}{B_2} \quad (4)$$

(5) Temporal change of width of torrent

$$\Delta B(\text{both banks}) \times H_1 = 2 \times ss_T \times \Delta t \times h_1$$

$$\frac{\partial B}{\partial t} = 2ss_T \cdot \frac{h_{s1}}{H_1} \quad (5)$$

(6) Erosion velocity rate of torrent bed

Erosion velocity equations are applied the equations find in Egashira et al. (Egashira et al., 1997) .

$$s_T = v_t \tan(\theta - \theta_e) \quad (6)$$

(7) Erosion velocity rate of torrent side bank

$$ss_T = \frac{1}{\alpha} \frac{h_{s1}}{H_1 + h_{s1}} v_t \quad (\alpha = 100 \sim 1,500) \quad (7)$$

where,  $\theta$ ; torrent gradient,  $\theta_e$ ; equilibrium gradient corresponding to the average density of the entire layer,  $B$ ; width,  $h$ ; thickness of the moving layer ( $h_w$ ; thickness of the water flow layer,  $h_s$ ; thickness of the gravel moving layer,  $h_t$ ; thickness of the entire moving layer),  $v$ ; mean velocity ( $v_s$ ; mean velocity of the gravel moving layer,  $v_w$ ; mean velocity of the water flow layer,  $v_t$ ; mean velocity of the entire moving layer),  $\gamma$ ; correction factors,  $c_s$ ; averaged sediment concentration of the gravel moving layer,  $c_* (=0.6)$ ; sediment concentration of the deposit layer,  $s_s$ ; volumetric values of the water flow layer per units of time and area through the interface, witch calculate as in the state of two layers defines  $c_s = c_*/2$ ,  $s_T$ ; erosion rate,  $ss_T$ ; velocity of side bank erosion,  $z_b$ ; torrent bed elevation,  $\alpha$ ; side erosion coefficient. Still, subscript  $1$  shows before bank erosion.

### Side bank erosion

Side bank erosion is applied discrives in Fig. 2.

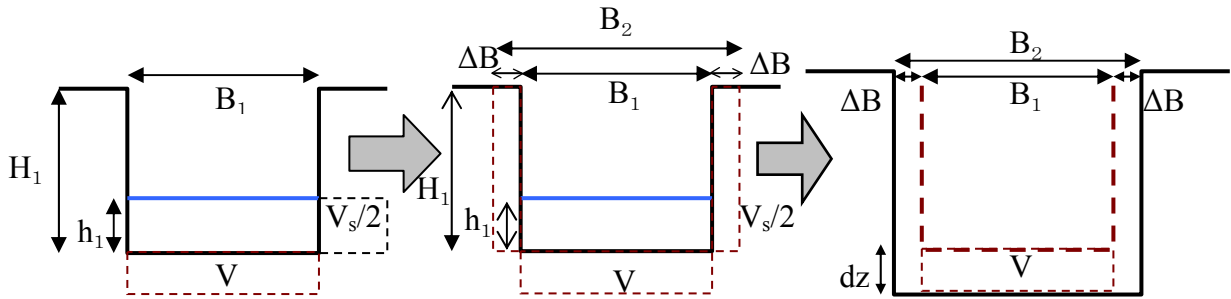


**Fig. 2** Schematic Diagram of bank erosion (Satofuka et al., 2007b)

where  $V$ ; erosion volume of torrent bed,  $V_s$ ; erosion volume of side bank,  $B_1$ ; primary width,  $B_2$ ; width of after side erosion,  $H_1$ ; primary depth of torrent,  $h_1$ ; flow depth,  $\Delta B$ ; erosion width of one side,  $dz$ ; fluctuate elevation of torrent bed.

## Equations of motion

### (1) Water flow layer

$$\frac{\partial(\rho_w v_w h_w)}{\partial t} + \frac{1}{B} \frac{\partial(\rho_w \beta_w v_w^2 B h_w)}{\partial x} - \rho_w s_l u_l = \rho_w g h_w \sin \theta - \frac{1}{B} \frac{\partial P_w}{\partial x} - P_l \frac{\partial h_s}{\partial x} - \tau_w \quad (8)$$

### (2) Gravel moving layer

$$\frac{\partial(\gamma' \rho_s v_s h_s)}{\partial t} + \frac{1}{B} \frac{\partial(\rho_s \beta_s v_s^2 B h_s)}{\partial x} + \rho_s s_l u_l = \rho_s g h_s \sin \theta - \frac{1}{B_1} \frac{\partial P_s}{\partial x} + P_l \frac{\partial h_s}{\partial x} + \tau_w - \tau_b \quad (9)$$

where  $\rho$ ; averaged density ( $\rho_s$ ; averaged density of the gravel moving layer,  $\rho_w$ ; averaged density of the water flow layer),  $g$ ; gravitational acceleration,  $u_x$ ;  $x$ -direction velocity at the interface,  $\tau_w$ ; shear stress to the interface,  $\tau_b$ ; shear stress to the torrent bed,  $P_w$ ; pressure acting the water layer integrated from the interface to the free surface,  $P_s$ ; pressure acting the gravel moving layer integrated from torrent bed to the interface,  $P_l$ ; pressure at the interface,  $\gamma'$ ,  $\beta_s$ ,  $\beta_w$ ; correction factors for the vertical distributions of velocity, sediment concentration and density respectively.

## Pressures

Pressures  $P_w$ ,  $P_s$  are rigidly describes below.

$$P_w = \frac{1}{2} \rho_w g h_w^2 \cos \theta \quad (10)$$

$$P_s = \rho_w (\sigma / \rho_w - 1) g h_s^2 \cos \theta \int_0^1 \left[ \int_z^1 c dz' \right] dz + \frac{1}{2} \rho_w g h_w (2h_w + h_s) \cos \theta \quad (11)$$

where  $z' = z / h_s$ ,  $c$  is sediment concentration, height  $z$  from torrent bed.

## Shear stress

The shear stress to the torrent bed are evaluated using the model found in Egashira et al. (Egashira et al., 1997) .

Composition rule are as follows.

$$\tau = \tau_y + \tau_f + \tau_d \quad (12)$$

$$p = p_w + p_s + p_d \quad (13)$$

$$\tau_y = p_s \tan \phi_s \quad (14)$$

$$\tau_f = \rho_w k_f \left\{ (1-c)^{5/3} / c^{2/3} \right\} d^2 (\partial u / \partial z)^2 \quad (15)$$

$$\tau_d = k_g \sigma (1-e^2) c^{1/3} d^2 (\partial u / \partial z)^2 \quad (16)$$

$$\partial p_w / \partial z = -\rho_w g \cos \theta \quad (17)$$

$$p_d = k_g \sigma e^2 c^{1/3} d^2 (\partial u / \partial z)^2 \quad (18)$$

$$p_s / (p_s + p_d) = (c / c_*)^{1/5} \quad (19)$$

where  $d$ ; mean diameter,  $\phi_s$ ; internal friction angle of the sediment ( $=35.0^\circ$ ),  $\sigma$ ; sediment density,  $\tau$ ; shear stress,  $p$ ; pressure,  $\tau_y$ ; surrender stress,  $\tau_f$ ; shear stress by the disorder of vacancy water,  $\tau_d$ ; shear stress by the un-elasticity collision of sediment particle,  $p_w$ ; pressure of the vacancy water,  $p_s$ ; stress of the particle frame,  $p_d$ ; pressure of the collision of sediment particle. The distribution revision coefficient assumed it 1 for simpleness and easiness entirely.  $k_f$ ,  $k_g$  are experienced constant value, witch are 0.25 and 0.0828 each, and  $e$  is repulsion factor ( $=0.85$ ).

Shear stress to the torrent bed as follows.

$$\tau_b = \tau_y + \rho_w f_s v_s |v_s| \quad (20)$$

$$\tau_y = \left( \frac{c_s}{c_*} \right)^{1/5} (\sigma - \rho_w) c_s g h_s \cos \theta \tan \phi_s \quad (21)$$

$$\tan \theta_e = \frac{(\sigma - \rho_w) c}{(\sigma - \rho_w) c + \rho_w} \tan \phi_s \quad (22)$$

$$G_{yk} = \frac{\tau_{ext}(z=z_k) - \tau_{yk}(z=z_k)}{\rho_w g h_s} = \{(\sigma/\rho_w - 1)c_s + 1\} \sin \theta_e - (\sigma/\rho_w - 1)c_s \cos \theta_e \left( \frac{c_s}{c_*} \right)^{1/5} \tan \phi_s \quad (23)$$

$$\eta_0 = \sqrt{k_f} \left( \frac{1 - c_s}{c_s} \right)^{1/3} d \quad (24)$$

$$W = \frac{\tau_w}{\rho_w g h_s} = \frac{f_w |v_w - u_l| (v_w - u_l)}{g h_s} \quad (25)$$

$$f_w = \left[ \frac{1}{\kappa} \left\{ \left( 1 + \frac{\eta_0}{h_w} \right) \ln \left( 1 + \frac{h_w}{\eta_0} \right) - 1 \right\} \right]^{-2} \quad (26)$$

$$f(c_s) = k_f \frac{(1 - c_s)^{5/3}}{c_s^{2/3}} + k_g \frac{\sigma}{\rho_w} (1 - e^2) c_s^{1/3} \quad (27)$$

when  $G_{yk} \neq 0$

$$f_s = \frac{225}{16} f(c_s) G_{yk}^4 (W + G_{yk}) \left\{ W^{5/2} - (W + G_{yk})^{3/2} \left( W - \frac{3}{2} G_{yk} \right) \right\}^{-2} \left( \frac{h_s}{d} \right)^{-2} \quad (28)$$

when  $G_{yk} = 0$

$$f_s = 4 f(c_s) \left( \frac{h_s}{d} \right)^{-2} \quad (29)$$

where  $\eta_0$ ; scale of the sediment particle vacancy,  $\tau_{ext}(Z=Z_b)$ ; shear stress for external force to the torrent bed,  $\tau_{yk}(Z=Z_b)$ ; surrender stress of directly upper surface of the torrent bed,  $\tau_b$ ; shear stress to the torrent bed,  $\kappa$ ; Karman's fixed number.

In case of torrent bed gradient are flat and resistance law for bed load transport is needed. We used Manning's resistance law when sediment concentration becomes less than 0.02 as Takahashi and Kuang did (Takahashi and Kuang., 1988).

$$\tau_b = \frac{\rho g n^2 v |v|}{h^{1/3}} \quad (30)$$

where  $n$  is Manning's roughness coefficient.

**The Tangjiashan landslide dam in Fu River, in the upper reaches of the Jialin River, a left-bank tributary of the Yangtze River in Sichuan Province, China in 2008**

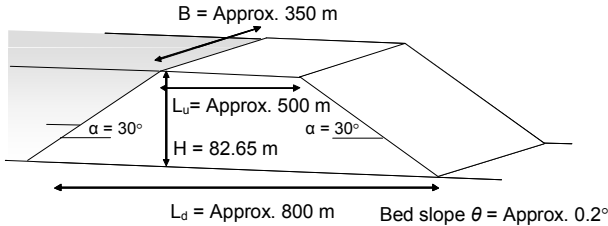
For the Tangjiashan landslide dam, which formed in Beichuan County, Sichuan Province due to the China Wenchuan Earthquake in May 2008, excavation of the crown was carried out by the People’s Liberation Army as a countermeasure against a potential burst-caused flood, which produced significant results.

Based on information obtained via the Internet and the 90 m mesh topographic data from the Shuttle Radar Topography Mission (SRTM-3) before the disaster, we estimated the flood discharge resulting from an overflow burst under the conditions shown in Table 1. Subsequently, we compared our result with the calculated estimate of the flood discharge with the excavation of the crown carried out.

**Table 1** Values used in the calculation

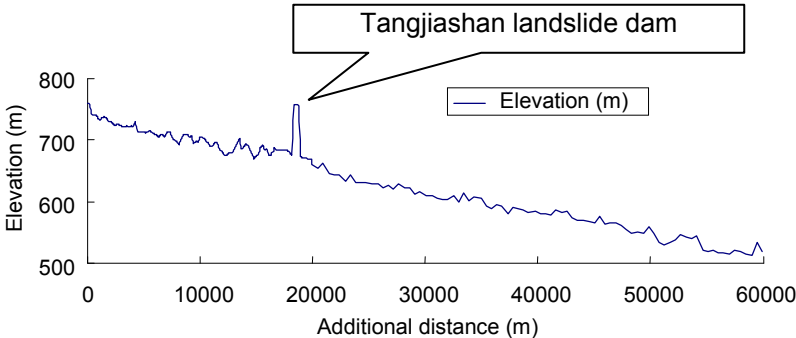
Water density	$\rho_w$	1.0 g/cm <sup>3</sup>
Gravel density	$\rho_s$	2.65 g/cm <sup>3</sup>
Average grain size	d	50 cm
Sediment layer density	c*	0.6
Internal friction angle	$\phi_s$	35°
Coefficient of restitution	e	0.85

As to the form of the landslide dam, a trapezoidal shape as shown in Fig. 3 was assumed.



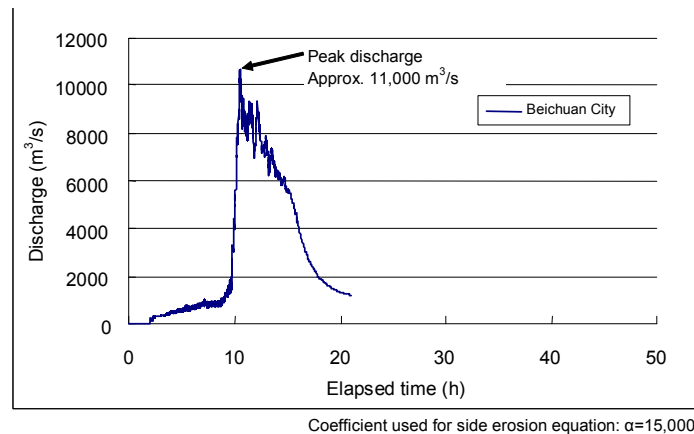
**Fig. 3** Shape of the Tangjiashan landslide dam used in calculation

The longitudinal profile of the river bed is as shown in Fig. 4.



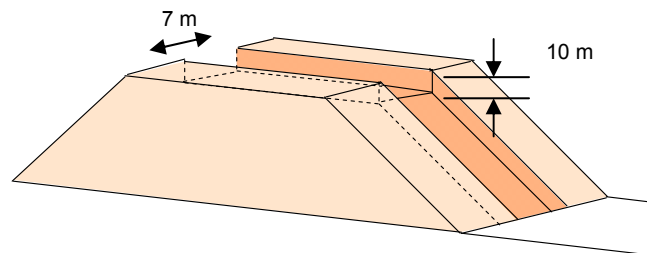
**Fig. 4** River bed longitudinal profile read from SRTM-3

Fig. 5 shows a flood hydrograph for Beichuan City of an overflow burst resulting from the natural overflow of the landslide dam. The peak discharge was approximately 11,000 m<sup>3</sup>/s.



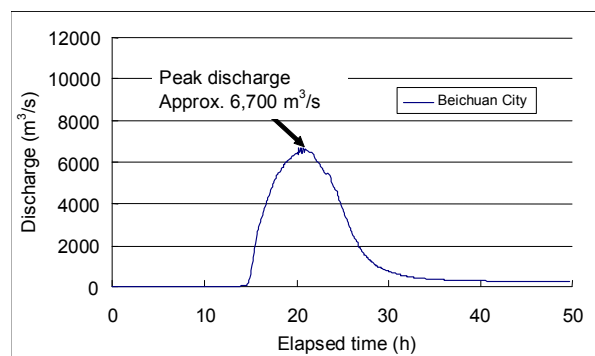
**Fig. 5** Flood hydrograph in the case of a natural overflow

For the Tangjiashan landslide dam, members of the People’s Liberation Army risked their lives in order to excavate a channel 10 m deep and 7 m wide at its base in the crown of the dam, which led to a successful overflow at an early stage. The dam body with the channel excavated was assumed to be as shown in Fig. 6 and the flood caused by the overflow burst was calculated accordingly.



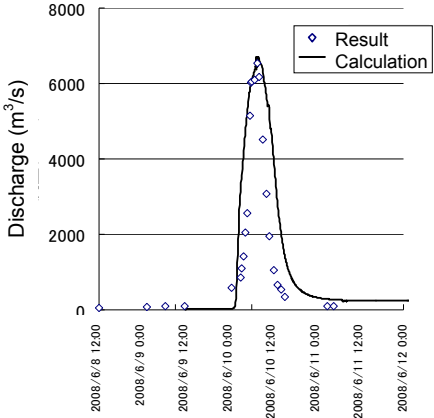
**Fig. 6** Dam body with channel excavated

Fig. 7 shows a hydrograph for Beichuan City downstream of the landslide dam. The peak discharge was calculated to be approximately 6,700 m<sup>3</sup>/s. This is almost equal to 6,500 m<sup>3</sup>/s mentioned in the May 2008 issue of the IAHR’s newsletter *Hydrolink*. (The value given in the April 2009 issue is 6,420 m<sup>3</sup>/s.)



**Fig. 7** Flood hydrograph with a channel excavated in crown

Fig. 8 shows the actual result of the flood obtained via the Internet overlapped with the calculation of the flood with a channel in place. The changes in the water level of the reservoir are also shown in Fig. 9 including the actual result as well as the calculation.



**Fig. 8** Flood discharge calculated values and actual results

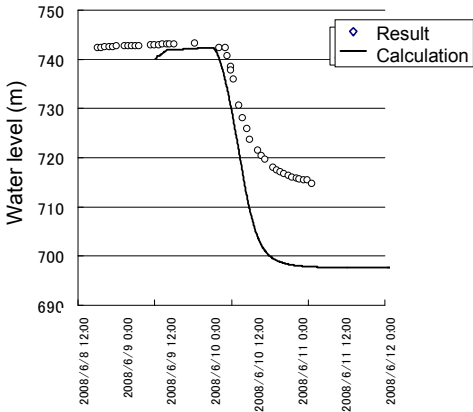


**Fig. 9** Change in water level

For the flood discharge, the actual result and the calculated result are roughly equal, although the peak duration according to the calculation is slightly longer. For the water level, the calculation shows a more remarkable reduction. This is apparently because that the total discharge is larger in the calculation, as is obvious from Fig. 8, and because large boulders contained in the dam body became entangled with each other to form an armor coat.

Fig.8 shows a result of a calculation with the side erosion coefficient ( $\alpha$ ) specified as 15,000. The results of calculations with  $\alpha$  specified as 1/10 of this value, or 1,500, and as ten times larger, or 150,000, are shown in Fig. 10 and Fig. 11, respectively, which yield significantly different results. The handling of the coefficient  $\alpha$  is an important factor in affecting the result.

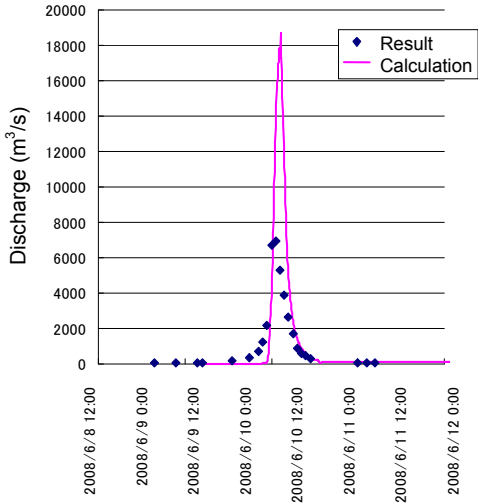


**Fig. 10** Calculation with  $\alpha = 1,500$

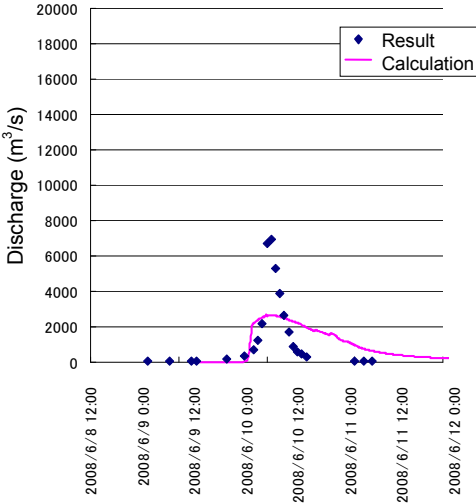


**Fig. 11** Calculation with  $\alpha = 150,000$

## Effect of channel excavation on the crown

For the Tangjiashan landslide dam, the size of the flood discharge was reduced through the excavation of a channel 7 m wide and 10 m deep into the crown. To help work out how the size of the flood generated can vary according to the width and depth of such a channel, we made calculations for six cases as listed in Table 2.

**Table 2** Calculation cases

	Excavation depth	Excavation width	Peak discharge
<b>Case 1</b>	<b>10</b>	<b>7</b>	<b>6,707 m<sup>3</sup>/s</b>
Case 2	5	7	8,502 m <sup>3</sup> /s
Case 3	20	7	4,753 m <sup>3</sup> /s
Case 4	10	3	7,261 m <sup>3</sup> /s
Case 5	10	14	6,776 m <sup>3</sup> /s
Case 6	10	20	6,875 m <sup>3</sup> /s

As a result, as shown in Fig. 12, we were able to confirm through our calculations that while varying the width (figure on the right) does not visibly alter the peak discharge reducing effect, increasing the depth (figure on the left) can produce a significant effect. This is apparently because the deeper excavation triggers the overflow sooner, reducing the amount of water retained upstream. Based on this result, we can say that for the purpose of reducing the value of the flood discharge resulting from the overflow burst of a landslide dam, lowering the crown of the landslide dam as much as possible or reducing the amount of water retained upstream of the dam as much as possible are effective measures.

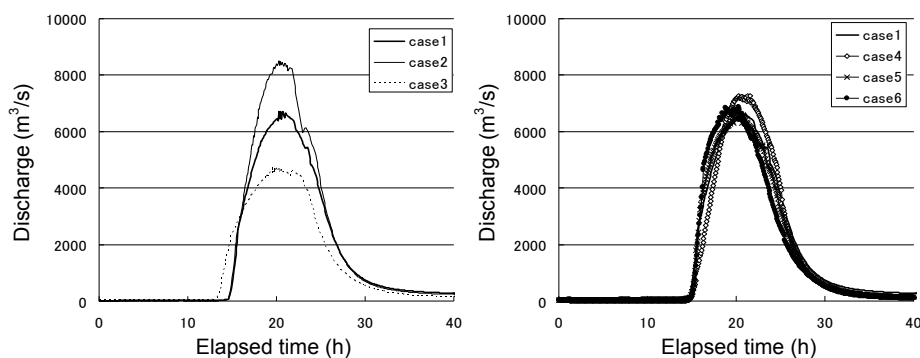


**Fig. 12** Change of flood discharge volume with changing excavation depth and width

## CONCLUSIONS

The authors applied an estimation method for flood hydrographs resulting from the overflow bursting of landslide dams based on the “two-layer model”, the practicality of which has been confirmed in Japan, to the Tangjiashan landslide dam formed in Wenchuan Earthquake that occurred in May 2008. The resulting simulation generally matched the reported actual result when using a value of 15,000 (1,000 to 1,500 for cases in Japan) as the side erosion coefficient. In addition, it has been confirmed by calculation that in the interests of reducing the flood discharge volume caused by overflow erosion, reducing the amount of inundation retained upstream is an effective method and the crown of the dam should be excavated at an early stage to generate overflow as soon as possible. The “two-layer model” may be rendered suitable for practical use following additional verification with further case examples and with compilation of the application method of parameters such as the side erosion coefficient into a

manual. In particular, information about the rough shape of a dam makes possible analysis of which of a large number of landslide dams formed simultaneously represent a danger to areas downstream, which the authors believe will be applicable to future crisis management.

When landslide dams form and burst in future, their forms before the burst and the flood level following the burst should be investigated and recorded for further verification of the two-layer model, and this can be expected to contribute to improved calculation accuracy.

## REFERENCES

- Chiba, M., Mori, T., Uchikawa, T., Mizuyama, T. and Satofuka, Y.(2007) : Bursting process of a landslide dam caused by Typhoon 14 (2005) in the Mimi River, Miyazaki Prefecture and suggestions on warning and evacuation when a landslide dam is formed, Journal of JSECE, Vol. 60, No. 1, p.43–47. (In Japanese with English abstract)
- Egashira, S., Miyamoto, K. and Ito, T. (1997): Bed load rate in view of two phase flow dynamics, Journal of Hydrosience and Hydraulic Engineering, Vol. 41, p. 789-794. (In Japanese with English abstract)
- Mizuyama, T., Satofuka, Y., Ogawa, K. and Mori, T.(2006): Estimating the outflow discharge rate from landslide dam outbursts, Proceedings of the INTERPRAEVENT International Symposium on Disaster Mitigation of Debris Flows, Slope Failures and Landslides, Vol. 1 of 2, p.365-377.(In English)
- Satofuka, Y., Yoshino, K., Ogawa, K., Mori, T., Mizuyama, T. and Takahama, J.(2007a): Simulation of a flood caused by the outburst of Takaiso-yama landslide dam, Journal of Japan Society of Erosion Control Engineering (JSECE), Vol. 59, No. 6, p. 32–37.(In Japanese with English abstract)
- Satofuka, Y., Yoshino, K., Mizuyama, T. Ogawa, K., Uchikawa, T. and Mori, T. (2007b): Prediction of floods caused by landslide dam collapse, Journal of Hydrosience and Hydraulic Engineering, Vol. 51, p. 901–906. (In Japanese with English abstract)
- Satofuka, Y., Yoshino, K., Ogawa, K. and Mizuyama, T. (2007c): Consideration on method of estimation for flood discharges caused by outburst of landslide dam, Journal of Japan Society of Erosion Control Engineering (JSECE), Vol. 59, No. 6, p.55-59.( In Japanese with English abstract)
- Takahama, J., Fujita, Y. and Kondo, Y. (2000) : Study on analysis method for migration from debris flow to hyperconcentrated flow, Journal of Hydrosience and Hydraulic Engineering, Vol. 44, p. 683–686. (In Japanese with English abstract)
- Takahashi, T. and Kuang, S. F. (1988): Hydrograph prediction of debris flow due to failure of landslide dam, Annuals Disaster Prevention Research Institute, Kyoto Univ., No. 31, B-2, p. 601-615. (In Japanese with English abstract)